The Emerald Research Register for this journal is available at
www.emeraldinsight.com/researchregister

The current issue and full text archive of this journal is available at
www.emeraldinsight.com/0961-5539.htm

Received April 2004
Revised January 2005
Accepted February 2005

A hybrid differencing scheme for mass transport in electrochemical systems

Kevin L. Heppner and Richard W. Evitts
Department of Chemical Engineering, University of Saskatchewan, Research Annex, Saskatoon, Saskatchewan, Canada

Abstract

Purpose – To present a new hybrid differencing scheme for the numerical solution of an electromigration-diffusion equation. The value of this work is evidenced by demonstrated improvement in the simulation of the Fu and Chan experiment when using the hybrid scheme.

Design/methodology/approach – A hybrid differencing scheme is developed which is based upon the solution of the pseudo-steady state electromigration-diffusion equation. In this scheme, a weighting parameter is calculated that varies the relative influence of the upwind node (relative to the direction of electromigration). This scheme significantly enhances the accuracy of electrochemical system mass transport models.

Findings – The hybrid scheme was compared to the upwind scheme. Use of the new hybrid scheme improved the accuracy of the model predictions by as much as 87 percent compared to the upwind scheme. However, use of the new scheme also increased the simulation time by between 6 and 43 percent. Deviations from electroneutrality and the presence of an activity coefficient gradient were detrimental to the stability of the hybrid scheme.

Research limitations/implications – This scheme is presented in the paper as an one-dimensional (1D) scheme. However, it could be extended to more than 1D but some artificial viscosity may result.

Practical implications – The hybrid scheme developed and demonstrated herein is useful for researchers developing mass transport models of electrochemical systems. It has been proven capable of improving the accuracy of electrolyte mass transport models.

Originality/value – This is the first hybrid differencing scheme designed for the special characteristics of electrochemical mass transport systems. It greatly improves the accuracy of simulation results. This work is useful to those who mathematically model electrochemical systems.

Keywords Modelling, Electromotive force, Transfer processes

Paper type Research paper

Nomenclature

C = molar concentration (mol/m^3)
D = diffusion coefficient (m^2/s)
F = Faraday's constant (96,487 C/mol)
G = rate of production or consumption via reactions (mol/s)
i = current density (A/m^2)
k_1 = constant of integration
k_2 = constant of integration
$\mathbf{N}$ = mass flux (mol/(m^2 s))
P = Peclet number
P' = Peclet number corrected for non-ideal solution behaviour
r_1 = root of quadratic expression
r_2 = root of quadratic expression
R = universal gas constant (8.3145 J/mol K)
t = time (s)
T = temperature (K)
u = mobility (m^2 mol/J s)
$\vec{v}$ = velocity (m/s)

International Journal of Numerical Methods for Heat & Fluid Flow
Vol. 15 No. 8, 2005
pp. 842-862
© Emerald Group Publishing Limited
0961-5539
DOI 10.1108/09615530510625110

x = spatial coordinate (m)
z = charge number

Greek letters
α = upwind parameter
β = constant of integration
γ = activity coefficient
δ = charge density (C/m^3)
ε = permittivity (Farad/m)
Φ = electrical potential (V)
κ = conductivity (S/m)
μ = chemical potential (J/mol)
$\tilde{\mu}$ = electrochemical potential (J/mol)
ξ = coefficient in
ψ = coefficient in (m^{-1})
ζ = coefficient in (m^{-2})
τ = constant of integration

Superscripts and subscripts
a = anion
c = cation
dp = diffusion potential
e = east interface
E = east node
i = index
j = index
P = point node
w = west interface
W = west node
0 = old value

1. Introduction

Considerable research effort has been focused upon technological areas in which the understanding of electrochemical kinetics coupled with electrolytic mass transport is of paramount importance. Such areas include corrosion control, energy generation via fuel cells, electrochemical separation techniques including ion exchange and electrophoresis, and electrochemical reactors. This research is focused upon the accurate modeling of electrolyte mass transport under the influence of an encompassing electrical field. A new differencing scheme for mass transport was developed and then validated against the moving boundary experiment (Fu and Chan, 1984).

Several differencing schemes have been developed for solving the convection-diffusion equation. The idea of an upwind differencing scheme (UDS) was first introduced by Courant *et al.* (1952) and subsequent work by Barakat and Clark (1966), Gentry *et al.* (1966) and Runchal and Wolfshtein (1969) followed. UDS replaces first-order derivative expressions with forward finite difference analogs. This scheme is appropriate for highly convective problems; only the upwind node influences the control volume. The central differencing scheme (CDS), appropriate for diffusive problems, employs central finite difference discretization thus equally dispersing influence to all physical control volume boundaries. Other schemes have since been developed which are appropriate where neither convection nor diffusion dominate. These schemes compromise between UDS and CDS based upon local physics (Patankar and Spalding, 1970; Spalding, 1972; Raithby and Torrence, 1974).

The electrolyte mass transport equation is unique from the convection-diffusion equation because an additional condition is added. Around each ion is a cloud of ions of opposing charge which, at equilibrium, exactly balance the space-averaged charge. However, when an electrolyte is a transport medium between two electrodes of differing electrical potential, a small portion of the Gibb's free energy that drives the coupled electrode charge transfer, mass transport, and chemical equilibrium process is stored in the electrolytic solution as charge density. Although small, the charge density has a large impact on the second order gradient of the electrical potential field; this feature induces significant instability in mass transport calculations. Therefore, ensuring a very small charge density in the solution is of paramount importance when simulating electrolytic mass transfer. In this work, mass transport is assumed to occur

in a solution of moderate dilution (Newman, 1973). The mass transport equation for such a solution is written as:

$$\frac{\partial C_i}{\partial t} = -z_i u_i F\left[\frac{\nabla C_i(\mathrm{i} + \mathrm{i}_{\mathrm{dp}})}{\kappa} + C_i\frac{\delta}{\varepsilon}\right] + D_i(\nabla^2 C_i + \nabla C_i \nabla \ln \gamma_i + C_i \nabla^2 \ln \gamma_i) + G_i \quad (1)$$

Equation (1) is the electromigration-diffusion transport equation and its solution is the focus of this work.

Accurately modeling electrolytic mass transport is essential when developing predictive models for localized corrosion. Previous authors have prescribed upwind parameters based upon the local Peclet number or have simply assumed electromigrative domination. Walton *et al.* (1996) modeled the crevice corrosion of type 304 stainless steel using UDS when the absolute value of the Peclet number was greater than two and CDS otherwise. Evitts (1997), Watson (1989), Watson and Postlethwaite (1990a, b, 1991) and Heppner *et al.* (2002) modeled the initiation of crevice corrosion in passive metals using UDS. To this point, no differencing scheme has been developed which uses an electromigration-diffusion balance equation to prescribe appropriate upwind parameters for mass transport under the influence of a potential gradient. For this reason, a HDS has been developed which varies the upwind parameter according to the solution of the pseudo-steady state electromigration-diffusion equation. This new differencing scheme enables more accurate prescription of the upwind parameter where neither electromigration nor diffusion dominates the mass transport process.

2. Development of the electrolyte mass transport hybrid differencing scheme

2.1 Background

The electrochemical potential gradient, which is composed of activity gradient and potential gradient contributions, is the sole driving force for mass transport of ions in a stagnant electrochemical system. In a moderately dilute solution, the transport of ions can be decomposed into two inter-coupled mechanisms:

(1) *Electromigration.* The transport of ionic species via an electrical potential gradient. Its mathematical form is similar to convection.

(2) *Diffusion.* The transport of ionic and neutral species along an activity gradient.

The upwind and downwind positions, referred frequently in the forthcoming discussion, represent the origin and destination, respectively, of ions driven by electromigration. Consider electromigration and diffusion balancing a chemical reaction source term at steady state in an infinitely dilute medium:

$$\left(z_i u_i F\frac{\mathrm{d}\Phi}{\mathrm{d}x}\right)\frac{\mathrm{d}C_i}{\mathrm{d}x} + D_i\frac{\mathrm{d}^2 C_i}{\mathrm{d}x^2} = G_i \quad (2)$$

As the potential gradient, $\mathrm{d}\Phi/\mathrm{d}x$, increases, the strength of electromigration relative to diffusion increases and the contribution of diffusion becomes insignificant:

$$\left(z_i u_i F\frac{\mathrm{d}\Phi}{\mathrm{d}x}\right)\frac{\mathrm{d}C_i}{\mathrm{d}x} = G_i \quad (3)$$

The solution of this first-order differential equation requires knowledge of only the upwind boundary. Thus, in regions of strong electromigration, the space-averaged concentration of ionic species in the control volume is highly dependent upon the concentration at the upwind boundary. In the absence of electromigration, both control volume boundaries have equal influence on the control volume. When the potential gradient is negligible, no electromigration occurs and (2) becomes:

$$D_i \frac{d^2 C_i}{dx^2} = G_i \tag{4}$$

Equation (4) is a form of the diffusion equation and conditions at both surrounding boundaries are required for its solution. Mathematically accounting for the dynamic boundary influence encountered in electrolytic mass transport problems requires the calculation of an upwind factor, a weighting parameter that adjusts the relative influence of the upwind node proportionate to the relative strength of electromigration versus diffusion. The upwind factor, α, modifies the interpolated value at an interface between two control volumes:

$$C_{i+(1/2)} = \frac{1+\alpha}{2} C_i + \frac{1-\alpha}{2} C_{i+1} \tag{5}$$

Here, i is a spatial node index. The mathematical description of α is based upon the solution of an electromigration-diffusion balance and its derivation follows.

2.2 Model derivation

The velocity of an ion migrating through an electrical field is (Newman, 1973):

$$v_i = -z_i u_i F \frac{d\Phi}{dx} \tag{6}$$

The velocity of an ion under the influence of pure diffusion is:

$$v_i = -\frac{D_i}{\Delta x} \tag{7}$$

The ratio of the two velocities gives a Peclet number for the electrolyte mass transport problem:

$$P = \frac{z_i u_i F \Delta x}{D_i} \frac{d\Phi}{dx} \tag{8}$$

The net mass flux across an arbitrary interface driven by an electrochemical potential gradient is described as:

$$\mathbf{N}_i = -\frac{D_i}{RT} C_i \nabla \tilde{\mu}_i \tag{9}$$

Assuming that moderately dilute solution theory is applicable, the electrochemical potential gradient can be segregated into an activity gradient (diffusion) and potential gradient (electromigration) contribution:

$$\mathbf{N}_i = -D_i \nabla C_i - D_i C_i \nabla \ln \gamma_i - z_i u_i F C_i \nabla \Phi \tag{10}$$

A pseudo-steady state mass balance on an infinitesimal one-dimensional (1D) control volume may be written:

$$\nabla \cdot \mathbf{N}_i = 0 \tag{11}$$

The pseudo-steady state assumption is valid provided that relatively small time steps are used. Equation (11) also assumes negligible chemical reaction – a valid assumption when chemical reactions occur much faster than mass transport. Substitution of (10) into (11) and subsequent application of the chain rule and rearrangement yields the following equation (in 1D):

$$\frac{\mathrm{d}^2 C_i}{\mathrm{d}x^2} + \left(\frac{z_i u_i F}{D_i}\frac{\mathrm{d}\Phi}{\mathrm{d}x} + \frac{\mathrm{d}\ln\gamma_i}{\mathrm{d}x}\right)\frac{\mathrm{d}C_i}{\mathrm{d}x} + \left(\frac{z_i u_i F}{D_i}\frac{\mathrm{d}^2\Phi}{\mathrm{d}x^2} + \frac{\mathrm{d}^2\ln\gamma_i}{\mathrm{d}x^2}\right)C_i = 0 \tag{12}$$

Poisson's equation for charge density describes the electrical potential distribution for a given electroneutrality condition:

$$\frac{\mathrm{d}^2\Phi}{\mathrm{d}x^2} = -\frac{\delta}{\varepsilon} \tag{13a}$$

where δ is the charge density:

$$\delta = F\sum_j z_j C_j \tag{13b}$$

Equation (13a) can be substituted into equation (12) to yield:

$$\frac{\mathrm{d}^2 C_i}{\mathrm{d}x^2} + \left(\frac{z_i u_i F}{D_i}\frac{\mathrm{d}\Phi}{\mathrm{d}x} + \frac{\mathrm{d}\ln\gamma_i}{\mathrm{d}x}\right)\frac{\mathrm{d}C_i}{\mathrm{d}x} + \left(-\frac{z_i u_i F}{D_i\varepsilon}\delta + \frac{\mathrm{d}^2\ln\gamma_i}{\mathrm{d}x^2}\right)C_i = 0 \tag{14}$$

By substitution of equation (8) into (14), this second order homogenous linear ordinary differential equation can be written in terms of the Peclet number:

$$\frac{\mathrm{d}^2 C_i}{\mathrm{d}x^2} + \left(\frac{P}{\Delta x} + \frac{\mathrm{d}\ln\gamma_i}{\mathrm{d}x}\right)\frac{\mathrm{d}C_i}{\mathrm{d}x} + \left(-\frac{z_i u_i F}{D_i\varepsilon}\delta + \frac{\mathrm{d}^2\ln\gamma_i}{\mathrm{d}x^2}\right)C_i = 0 \tag{15}$$

Equation (15) can then be expressed as:

$$\xi\frac{\mathrm{d}^2 C_i}{\mathrm{d}x^2} + \psi\frac{\mathrm{d}C_i}{\mathrm{d}x} + \zeta C_i = 0 \tag{16}$$

where:

$$\xi = 1$$

$$\psi = \frac{P}{\Delta x} + \frac{\mathrm{d}\ln\gamma_i}{\mathrm{d}x}$$

$$\zeta = -\frac{z_i u_i F}{D_i\varepsilon}\delta + \frac{\mathrm{d}^2\ln\gamma_i}{\mathrm{d}x^2}$$

The over-damped solution of equation (16) is the desired physically realistic non-oscillatory solution. This occurs when $\psi^2 > 4\xi\zeta$. To ensure that the problem is always over-damped, two assumptions are made to eradicate the coefficient, ζ:

(1) Any charge separation in an electrolytic solution invokes powerful forces that quickly reinstate electroneutrality. Outside of the electrical double layer region which is located very near an electrochemically reactive wall (such as a corroding metal surface), it is reasonable to assume an electrically neutral system ($\delta = 0$).

(2) Where activity coefficient gradients do not vary significantly, it can be assumed that the second order derivative of the activity coefficient is zero ($d^2 \ln \gamma_i / dx^2 = 0$).

With these two assumptions, the coefficient, ζ, can be neglected:

$$\zeta = -\frac{z_i u_i F}{D_i \varepsilon}\delta + \frac{d^2 \ln \gamma_i}{dx^2} = 0 \tag{17}$$

A non-oscillatory solution is then guaranteed across each computational node.

Now consider one computational control volume across which the particular solution to the ordinary differential equation can be obtained. At the western interface ($x = 0$), the concentration is equal to $C_{i\mathrm{w}}$ while at the eastern interface ($x = \Delta x$), the concentration is $C_{i\mathrm{e}}$. Through application of these boundary conditions, the particular solution of the second order problem is obtained:

$$C_i(x) = C_{i\mathrm{w}} + (C_{i\mathrm{e}} - C_{i\mathrm{w}})\frac{e^{-\frac{\psi}{\xi}x} - 1}{e^{-\frac{\psi}{\xi}\Delta x} - 1} \tag{18}$$

Substituting the definition of ξ and ψ gives the final form of the solution:

$$C_i(x) = C_{i\mathrm{w}} + (C_{i\mathrm{e}} - C_{i\mathrm{w}})\frac{e^{-P'\frac{x}{\Delta x}} - 1}{e^{-P'} - 1} \tag{19a}$$

where:

$$P' = P + \frac{d \ln \gamma_i}{dx}\Delta x \tag{19b}$$

Equation (19b) shows that the magnitude of the activity coefficient gradient has a direct effect on the dominance of electromigration in electrolyte mass transport problems. The activity coefficient gradient accounts for the influence of other ions in solution of the ith ion. It is the force that propels the ion towards regions of lower ionic strength. From equation (19a), the concentration at the center of the control volume is then:

$$C_{i\mathrm{P}} = C_{i\mathrm{w}} + (C_{i\mathrm{e}} - C_{i\mathrm{w}})\frac{e^{-\frac{P'}{2}} - 1}{e^{-P'} - 1} \tag{20}$$

By assuming an upwinding function of the form:

$$C_{i\mathrm{P}} = \left(\frac{1+\alpha}{2}\right)C_{i\mathrm{w}} + \left(\frac{1-\alpha}{2}\right)C_{i\mathrm{e}} \tag{21}$$

Equations (20) and (21) can be solved simultaneously to yield a formula for α:

$$\alpha = 1 - 2\left(\frac{e^{-\frac{P'}{2}} - 1}{e^{-P'} - 1}\right) \tag{22}$$

When the charge density and second order derivative of the activity coefficient is assumed negligible, the resulting upwind parameter formula is similar to the exponential differencing scheme (Spalding, 1972; Raithby and Torrence, 1974). However, unlike convective problems where the Peclet number (Reynolds number) is dependent only upon the velocity and viscosity of the fluid, the electrolyte mass transport Peclet number is dependent upon the velocity of the ion under the influence of an electrical field, the diffusivity, and the magnitude of the activity coefficient gradient. This is an 1D scheme which can be applied to multidimensional problems. However, application of an 1D scheme to 2D and 3D problems will introduce artificial viscosity effects (Raithby and Schneider, 1980). This phenomenon may be controlled through grid refinement. The spatial upwind parameter profile is shown for a range of Peclet numbers in Figure 1.

There are cases where the assumptions used to obtain equation (22) are not valid. Two examples are the modeling of transport in regions of strong-coupled electromigration and diffusion, where charge density cannot be neglected, and in electromigration-dominated problems where the activity coefficient gradient may vary significantly in space. In these cases, equation (22) should not be used. Instead, the value of $(\psi^2 - 4\xi\zeta)$ should be determined and, based upon its sign, the appropriate solution to the ordinary differential equation (under-damped, over-damped, or critically damped) should be selected. Then, $C_{i\,\mathrm{P}}$, $C_{i\mathrm{e}}$, and $C_{i\mathrm{w}}$ may be calculated. The appropriate value for α can be obtained through rearrangement of equation (21):

$$\alpha = \frac{C_{i\mathrm{w}} + C_{i\mathrm{e}} - 2C_{i\mathrm{P}}}{C_{i\mathrm{e}} - C_{i\mathrm{w}}} \tag{23}$$

Depending upon the size of the second order derivative of the activity coefficient, and in particular, the charge density, the predicted upwind parameter may not be physically realistic (the solution may be under-damped). The following section

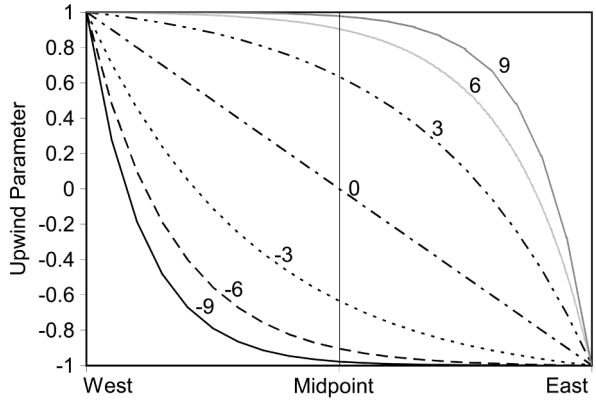

Figure 1.
The spatial upwind parameter profile across a computational control volume over a range of peclet numbers

demonstrates the effect of charge density on the stability of the mass transport problem.

2.3 Stability of the electrolyte mass transport hybrid differencing scheme

Unlike the convection-diffusion equation, the electromigration-diffusion mass transport problem is influenced by an electrical field. The mass transport problem is therefore governed by the following condition: unless a very large amount of work is done on the system, the solution must possess negligible charge density. To obtain the exponential formula for the upwinding parameter previously presented, the solution charge density was assumed to be negligible. For this assumption to be valid, care must be taken to ensure that the numerical solution algorithm respects the electroneutrality condition inherent to the mass transport mechanism. If the charge density tolerance during the numerical solution of the mass transport equation is too high, the steady state balance between electromigration and diffusion will become under-damped. The particular solution of the under-damped electromigration-diffusion balance equation ($\psi^2 < 4\xi\zeta$) is:

$$C_i(x) = e^{\tau x}\left\{C_{iw}\cos(\beta x) + [C_{ie}e^{-\tau\Delta x} - C_{iw}\cos(\beta\Delta x)]\frac{\sin(\beta x)}{\sin(\beta\Delta x)}\right\} \tag{24a}$$

where the real and imaginary components, respectively, of the complex conjugate roots of the characteristic equation are:

$$\tau = -\frac{\psi}{2\xi} \tag{24b}$$

$$\beta = \frac{\sqrt{(4\xi\zeta - \psi^2)}}{2\xi} \tag{24c}$$

This solution predicts a sinusoidal concentration profile across the computational control volume and is clearly physically unrealistic. Figure 2 shows the predicted control volume concentration profile for a range of very small charge densities. As the charge density increases, the solution becomes under-damped; the increasingly sinusoidal concentration profile causes physically unrealistic predictions of the upwind parameter.

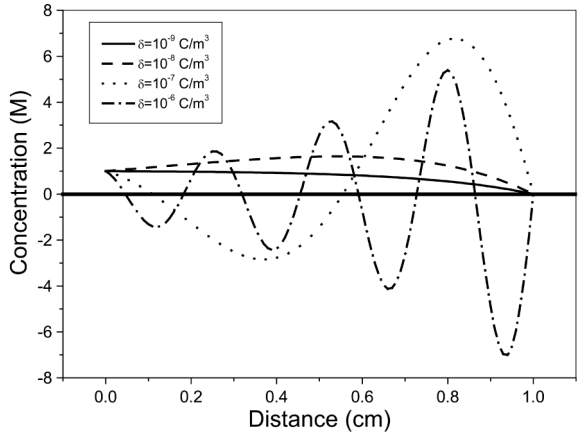

Figure 2.
Solution of the electromigration-diffusion balance equation across a computational control volume as solution charge density increases. Critical damping occurs when $\delta \approx 7.7 \times 10^{-9}\,\mathrm{C/m^3}$

When numerically based or artificial charge density is present, equation (14) shows that the concentration profile is now dependent upon not only the gradient of the concentration field but also on the value of the concentration. This introduces new instability problems – as the concentration profile rises or falls, the profile will mutate to an extent proportionate to the level of charge density in solution. Figure 3 shows this effect. Figure 3(a) shows that the shape of the concentration profile is invariant with the value of concentration for an electrically neutral system. However, even before the critical damping charge density (approximately $7.7 \times 10^{-9}\,\mathrm{C/m^3}$ for this example) is surpassed, the concentration profile begins to bulge beyond the electrically neutral profile, a feature that is exaggerated as the concentration profile boundary conditions are increased. Where the concentration profile extends beyond the range $[C(x = 0),\ C(x = \Delta x)]$, the predicted upwind parameter will lie outside of [-1, 1]. An acceptable value of the upwind parameter lies in the range [-1, 1]. Figure 3(c) is a slightly under-damped system. Examination of equation (24a) shows that the real component of the complex conjugate roots of the characteristic equation, τ, determines the amplitude while β, the imaginary component of the roots, controls the frequency. Because β is relatively small to τ, the period of the oscillation is greater than Δx and the sinusoidal influence is not observable. As the value of the boundary conditions are increased, the concentration profile extends well beyond $[C(x = 0),\ C(x = \Delta x)]$ and unrealistic values of the upwind parameter will be predicted. In Figure 3(d), the frequency of the oscillations has increased due to the increased imaginary component of the complex conjugate roots. The sinusoidal component of the mass balance equation solution dominates and an unrealistic sinusoidal concentration profile is observed. The amplitude of the oscillations increases as the concentration profile is raised.

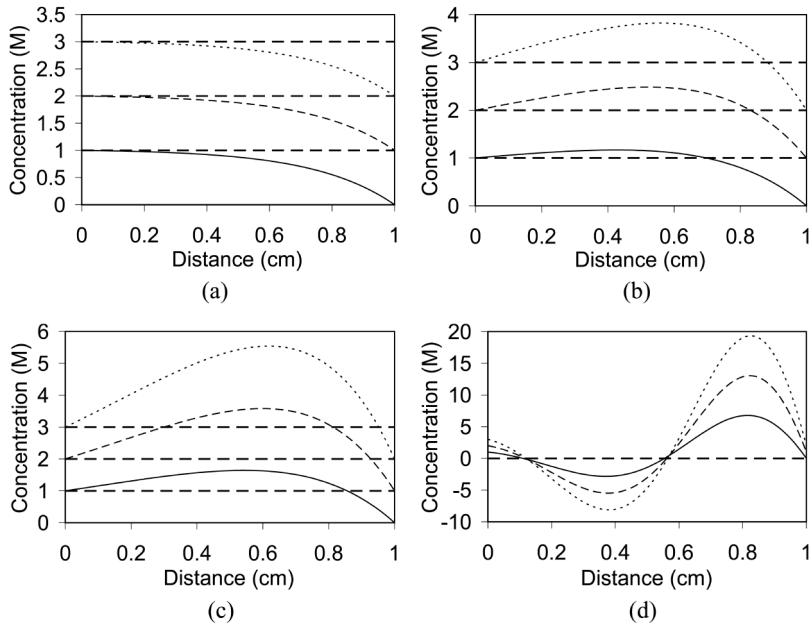

Figure 3.
Solution of the electromigration-diffusion balance equation across a computational control volume as the concentration profile is shifted upwards; a) $\delta = 0\,\mathrm{C/m^3}$; b) $\delta = 5 \times 10^{-9}$; c) $\delta = 1 \times 10^{-8}\,\mathrm{C/m^3}$; c) $\delta = 1 \times 10^{-7}\,\mathrm{C/m^3}$. Critical damping occurs when $\delta \approx 7.7 \times 10^{-9}\,\mathrm{C/m^3}$

Results presented in the preceding discussion show that even slight charge density arising in the numerical solution algorithm is detrimental to the fidelity of the predicted upwind parameter. This feature makes electrolyte mass transport unique from other forms of transport and adds an additional concern when developing codes for its prediction. A method has been developed by Heppner *et al.* (2002) to eradicate charge density in an electrolyte solution.

3. Discrete transport model development

Transport of ions and neutral species in a moderately dilute electrolyte solution under the influence of an electrochemical potential gradient can be described by:

$$\frac{\partial C_i}{\partial t} = -z_i u_i F\left[\frac{\nabla C_i(i + i_{\mathrm{dp}})}{\kappa} + C_i\frac{\delta}{\varepsilon}\right] + D_i(\nabla^2 C_i + \nabla C_i \nabla \ln \gamma_i + C_i \nabla^2 \ln \gamma_i) + G_i \quad (25)$$

where the current density induced by diffusion potential is:

$$i_{\mathrm{dp}} = F\sum_{j=1}^{k} z_j D_j(\nabla C_j + C_j \nabla \ln \gamma_j) \quad (26)$$

and the local net charge of the solution is given by equation (13b). Discretization using central finite difference approximations to first- and second-order derivatives, respectively, transforms (25) and (26) to a second order accurate analog form:

$$\begin{aligned}\frac{C_{i\mathrm{P}} - C^0_{i\mathrm{P}}}{\Delta t} = {} & -z_i u_i F\left[\frac{C_{i\mathrm{e}} - C_{i\mathrm{w}}}{\Delta x}\frac{i_{\mathrm{P}} + i_{\mathrm{dpP}}}{\kappa_{\mathrm{P}}} + C_{i\mathrm{P}}\frac{\delta_P}{\varepsilon}\right] \\ & + D_i\left(\begin{array}{l}\dfrac{C_{i\mathrm{E}} + C_{i\mathrm{W}} - 2C_{i\mathrm{P}}}{\Delta x^2} + \dfrac{(C_{i\mathrm{e}} - C_{i\mathrm{w}})(\ln \gamma_{i\mathrm{E}} - \ln \gamma_{i\mathrm{W}})}{2\Delta x^2} \\ \\ + C_{i\mathrm{P}}\dfrac{\ln \gamma_{i\mathrm{E}} + \ln \gamma_{i\mathrm{W}} - 2\ln \gamma_{i\mathrm{P}}}{\Delta x^2}\end{array}\right) + G_{i\mathrm{P}}\end{aligned} \quad (27)$$

$$i_{\mathrm{dp}} = F\sum_{j=1}^{k} z_j D_j\left(\frac{C_{j\mathrm{e}} - C_{j\mathrm{w}}}{\Delta x} + C_{j\mathrm{P}}\frac{\ln \gamma_{j\mathrm{e}} - \ln \gamma_{j\mathrm{w}}}{\Delta x}\right) \quad (28)$$

The P, E, and W nodes in this fully implicit discrete transport equation are the point, east and west nodes, respectively. The e and w subscripts denote the east and west control volume interfaces, respectively, located halfway between the surrounding nodes for a uniform grid. The expression of interfacial properties – $C_{i\mathrm{e}}$, $C_{i\mathrm{w}}$, $\ln \gamma_{i\mathrm{e}}$, and $\ln \gamma_{i\mathrm{w}}$ – as functions of nodal values is accomplished using the upwind parameter formulation, i.e.:

$$C_{i\mathrm{e}} = \frac{1 + \alpha}{2}C_{i\mathrm{P}} + \frac{1 - \alpha}{2}C_{i\mathrm{E}} \quad (29)$$

Substitutions analogous to equation (29) are made for each interfacial property appearing in equation (27) to yield the following discrete mass transport equation:

$$\frac{C_{i\mathrm{P}} - C_{i\mathrm{P}}^{0}}{\Delta t} = -z_i u_i F \left[\begin{array}{l} \dfrac{\frac{1+\alpha}{2} C_{i\mathrm{P}} + \frac{1-\alpha}{2} C_{i\mathrm{E}} - \frac{1+\alpha}{2} C_{i\mathrm{W}} - \frac{1-\alpha}{2} C_{i\mathrm{P}}}{\Delta x} \dfrac{i_{\mathrm{P}} + i_{\mathrm{dpP}}}{\kappa_{\mathrm{P}}} \\ + C_{i\mathrm{P}} \dfrac{\delta_{\mathrm{P}}}{\varepsilon} \end{array} \right] + D_i \left(\begin{array}{l} \dfrac{C_{i\mathrm{E}} + C_{i\mathrm{W}} - 2C_{i\mathrm{P}}}{\Delta x^2} + \dfrac{(C_{ie} - C_{iw})(\ln \gamma_{i\mathrm{E}} - \ln \gamma_{i\mathrm{W}})}{2\Delta x^2} \\ + C_{i\mathrm{P}} \dfrac{\ln \gamma_{i\mathrm{E}} + \ln \gamma_{i\mathrm{W}} - 2 \ln \gamma_{i\mathrm{P}}}{\Delta x^2} \end{array} \right) + G_{i\mathrm{P}} \tag{30}$$

By sequestering time-step lagged non-linear terms into transport coefficients, equation (30) can be rearranged into a linear algebraic discrete transport equation which is solved iteratively:

$$a_{\mathrm{P}} C_{i\mathrm{P}} = a_{\mathrm{E}} C_{i\mathrm{E}} + a_{\mathrm{W}} C_{i\mathrm{W}} + a_{\mathrm{P}}^{0} C_{i\mathrm{P}}^{0} + G_i \Delta x \tag{31}$$

Using the proposed hybrid differencing scheme to express the interfacial concentrations, C_{ie} and C_{iw}, as nodal values, the discrete transport coefficients are:

$$a_{\mathrm{E}} = \frac{D_i}{\Delta x} \left[1 + \frac{P_P^{'}}{2} + \left| \frac{P_P^{'} \alpha}{2} \right| \right] \tag{32}$$

$$a_{\mathrm{W}} = \frac{D_i}{\Delta x} \left[1 - \frac{P_P^{'}}{2} + \left| \frac{P_P^{'} \alpha}{2} \right| \right] \tag{33}$$

$$a_P^{0} = \frac{\Delta x}{\Delta t} \tag{34}$$

$$a_P = a_{\mathrm{E}} + a_{\mathrm{W}} + a_P^{0} + z_i u_i F \frac{\delta_P}{\varepsilon} \Delta x - D_i \frac{\ln \gamma_{i\mathrm{E}} + \ln \gamma_{i\mathrm{W}} - 2 \ln \gamma_{i\mathrm{P}}}{\Delta x} \tag{35}$$

where the local Peclet number, $P_{\mathrm{P}}^{'}$, is defined in equation (19b). The diffusion potential current density, equation (28), is also recast in terms of nodal values using the upwind formulation. After rearrangement, the following expression results:

$$i_{\mathrm{dp}} = F \sum_{j=1}^{k} z_j D_j \left(\begin{array}{l} \dfrac{2\alpha C_{j\mathrm{P}} + C_{j\mathrm{E}} - C_{j\mathrm{W}} - \alpha(C_{j\mathrm{E}} + C_{j\mathrm{W}})}{2\Delta x} \\ + C_{j\mathrm{P}} \dfrac{2\alpha \ln \gamma_{j\mathrm{P}} + \ln \gamma_{j\mathrm{E}} - \ln \gamma_{j\mathrm{W}} - \alpha(\ln \gamma_{j\mathrm{E}} + \ln \gamma_{j\mathrm{W}})}{2\Delta x} \end{array} \right) \tag{36}$$

Patankar (1980) stated that to ensure a physically realistic solution, the point coefficient should be the sum of the east, west, and previous iteration point coefficient and each coefficient should be positive. This mass transport model follows not only Patankar's suggestion but also contains non-linear influence from a net solution charge

imbalance, δ_P, and the second order derivative of the activity coefficient. The point coefficient is extremely sensitive to this charge imbalance which can possess a positive or negative value. A negative δ_P will reduce the diagonal dominance of the solution matrix. Furthermore, it is shown in Figure 2 that a charge imbalance will cause the hybrid differencing scheme to give unrealistic upwind parameters. The second order activity coefficient gradient will also have an effect on the convergence of the mass transport problem. If the second order gradient of the activity coefficient is positive in sign, it will increase the diagonal dominance and the speed of convergence of the system. Conversely, a positive second order gradient of the activity coefficient will decrease the diagonal dominance. A diagonally dominant linear system satisfies the Scarborough criterion and is guaranteed to converge by the Gauss-Seidel method. The Scarborough criterion is (Scarborough, 1958):

$$\frac{|a_{\mathrm{E}}| + |a_{\mathrm{W}}|}{|a_{\mathrm{P}}|} \begin{cases} \leq 1 & \text{(for all grid points)} \\ < 1 & \text{(for one grid point)} \end{cases} \tag{37}$$

The diagonal dominance of the coefficient matrix is largely controlled by a_{P}^0 – decreasing the time step increases a_{P}^0 and the point coefficient, a_{P}. However, if the charge density and/or the second order activity gradient is significant, extremely small time steps may be required to negate these influences and ensure satisfaction of (37) (Heppner *et al.*, 2002). The charge density term in the a_P coefficient formulation is extremely sensitive to charge density. Therefore, to ensure the diagonal dominance of the matrix, Heppner *et al.* recommended the removal of the electroneutrality deviation term from the a_p coefficient through an operator splitting strategy (Heppner *et al.*, 2002). After removal of the charge density term, the Scarborough Criterion for the variable UDS can be shown to be:

$$\frac{|a_{\mathrm{E}}| + |a_{\mathrm{W}}|}{|a_{\mathrm{P}}|} = \frac{1}{1 + \frac{1}{2 + P_{\mathrm{P}}^{'}\alpha}\left(\frac{\Delta x^2}{D_i \Delta t} - \ln \gamma_{i\mathrm{E}} - \ln \gamma_{i\mathrm{W}} + 2 \ln \gamma_{i\mathrm{P}}\right)} \tag{38}$$

Equation (38) is bounded between 0 and 1 when:

$$0 \leq \frac{1}{2 + P_{\mathrm{P}}^{'}\alpha}\left(\frac{\Delta x^2}{D_i \Delta t} - \ln \gamma_{i\mathrm{E}} - \ln \gamma_{i\mathrm{W}} + 2 \ln \gamma_{i\mathrm{P}}\right) \leq \infty \tag{39a}$$

or when:

$$-\infty \leq \frac{1}{2 + P_{P}^{'}\alpha}\left(\frac{\Delta x^2}{D_i \Delta t} - \ln \gamma_{i\mathrm{E}} - \ln \gamma_{i\mathrm{W}} + 2 \ln \gamma_{i\mathrm{P}}\right) \leq -2 \tag{39b}$$

Therefore, the Scarborough criterion is not bounded between 0 and 1 when:

$$-2 < \frac{1}{2 + P_{P}^{'}\alpha}\left(\frac{\Delta x^2}{D_i \Delta t} - \ln \gamma_{i\mathrm{E}} - \ln \gamma_{i\mathrm{W}} + 2 \ln \gamma_{i\mathrm{P}}\right) < 0 \tag{39c}$$

Condition (39a) would be guaranteed if (x_{E}, $\ln \gamma_{i\,\mathrm{E}}$) ($x_{\mathrm{W}}$, $\ln \gamma_{i\,\mathrm{W}}$), and ($x_P$, $\ln \gamma_{i\,\mathrm{P}}$) were points on a linear function. However, if $\ln \gamma_i$ possesses a non-zero second order gradient

over the range [x_W, x_E],condition (39a) may not be satisfied. The second order gradient of the activity coefficient is capable of inducing instability through reduction of diagonal dominance in the mass transport calculation procedure. To ensure that the Scarborough Criterion is satisfied, the time step should be lowered where the second order gradient of the activity coefficient is significant and positive in sign. If condition (39a) or (39b) is met, and if Dirichlet conditions exist at any physical domain boundary, the discrete mass transport problem satisfies the Scarborough Criterion. Figure 4 shows the east transport coefficient divided by $D_i/\Delta x$ against the Peclet number. The west coefficient is the mirror image of the east coefficient reflected across the y-axis. By Figure 4, it is shown that the east and west transport coefficients will never acquire a negative value.

4. Modeling of the Fu and Chan moving boundary experiment

Fu and Chan placed a silver anode plug at one end of a long glass tube. The tube opened into a large beaker in which a silver cathode was immersed. Initially, the entire apparatus was filled with a 0.1 M KNO_3 solution. A current density of 318 $\mu A/cm^2$ was applied across the tube length inducing silver dissolution at the anode plug and silver plating at the cathode. The electrical current forced Ag^+ and K^+ ions out of the tube towards the cathode while NO_3^- ions were driven towards the silver anode plug. A visible moving boundary was formed where the aqueous solution transitioned from being predominantly KNO_3 to being predominantly $AgNO_3$. The rate of movement of this boundary indicated the rate of mass transport in the tube. Fu and Chan accurately recorded the position of the moving boundary. Using data obtained from the moving boundary experiment performed by Fu and Chan (1984), the ability of this hybrid differencing scheme to improve the physical realism of solutions of the electrolyte mass transport equation is showcased.

Using the present transport model, the boundary region predicted using UDS and HDS is compared. For both differencing schemes, the solution domain was discretized into 1,000 nodes ($\Delta x = 5 \times 10^{-3}$ cm) and a time step of 0.1 s was used. The solution algorithm is shown as a flow chart in Figure 5.

Figure 6 shows the predicted moving boundary region after 5, 20, 30, and 40 min using both UDS and HDS. The vertical line in each figure represents the position of the boundary at the respective time (interpolated from raw data) observed experimentally

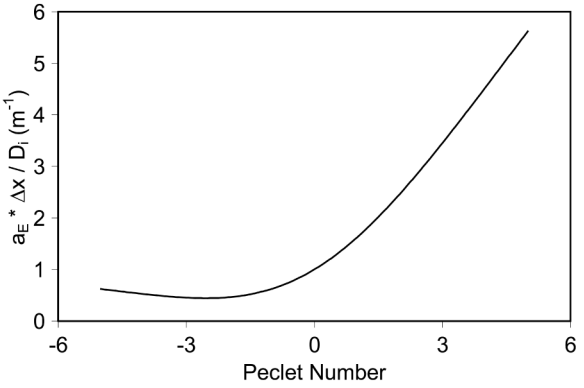

Figure 4.
The variation of $a_E \Delta x/D_i$ with the Peclet number

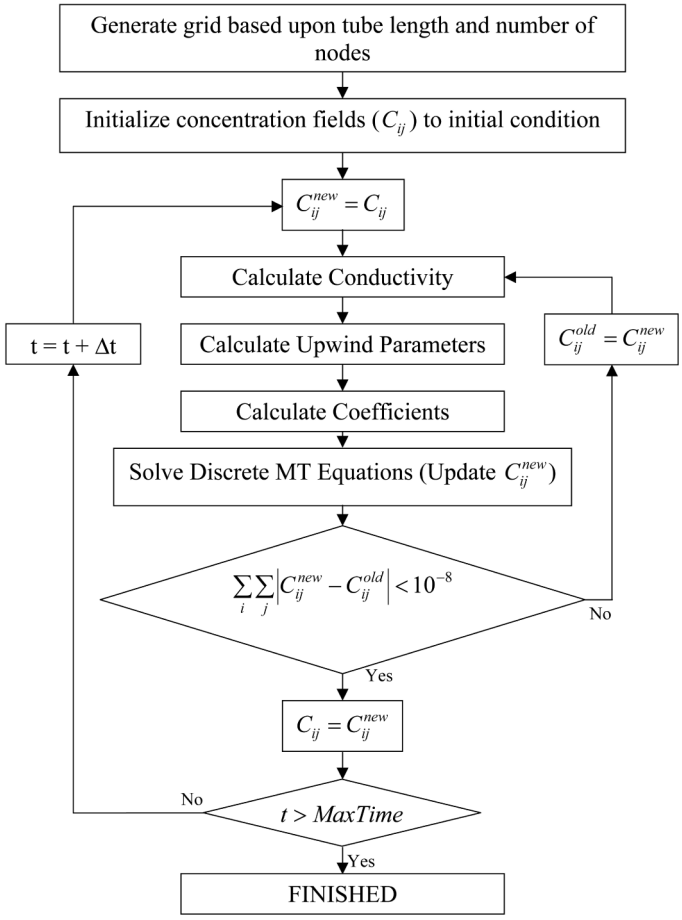

Figure 5.
The mass transport model solution algorithm presented as a flow sheet

by Fu and Chan. At each time, discretizing the mass transport model using HDS, rather than UDS, results in the formation of steeper concentration gradients, and thus faster mass transport rates, throughout the moving boundary region. The fact that using HDS predicts increased mass transfer rates is evidenced by both the faster movement of the predicted Ag^+/K^+ concentration profile intersection, and by a lower $AgNO_3$ concentration at the anode-solution interface (not seen in figure). Comparison of Figure 6(a) and (b) shows that sometime between 5 and 20 min after the start of the simulation, the moving boundary predicted using HDS passes the moving boundary predicted using UDS. In each case, the mass transport model discretized using HDS either matches or improves on the accuracy of the same transport model discretized using UDS. The average error between the predicted boundary position and that measured experimentally has decreased by 61 percent by using HDS rather than UDS. The greatest increase in accuracy is seen in Figure 6(d) where the error decreased by 87 percent. Using the new differencing scheme enables the discrete mass transport model to more accurately predict the experimental observations of Fu and Chan.

4.1 Effect of charge density

The previous section showed the ability of the discrete mass transport model coupled with the HDS upwind parameter solver to accurately predict mass transport in an electrolytic system. Inherent to HDS is the assumption of electroneutrality throughout the system. Although a physical system will not possess an appreciable charge density unless a substantial amount of work is done on the system, numerical charge density arising through solution of the constitutive mass conservation equations can cause oscillations in the solution of the electromigration-diffusion balance equation. Obviously, predicted concentration profiles that are sinusoidal and feature negative values are not physically realistic. Therefore, one cannot expect to obtain a physically meaningful value of the upwind parameter from such a profile. The sensitivity of the numerical solution to accumulated charge density in the solution is now tested. Figure 7 shows the predicted moving boundary region as the amount of charge density in the solution is increased. Increased charge density had a large effect on the stability of the numerical algorithm. As the charge density was increased, the mass transport equation became more difficult to solve. When the charge density was set to 10^{-9} C/m^3 or greater, the solution to the migration-diffusion equation became under-damped and the simulation ultimately failed to converged. When the charge density reached a value such that it caused under-damping of the predicted concentration profile, the simulation immediately failed. However, until the profile became critically damped, the simulation was able to proceed but provided results with significant amounts of error.

4.2 Effect of spatial step size

As the spatial step size is decreased, the predicted concentration profiles approach the exact solution to the constitutive equations. However, decreasing the step size also affects the predicted Peclet number and, thus, the upwind parameter. Figure 8 shows

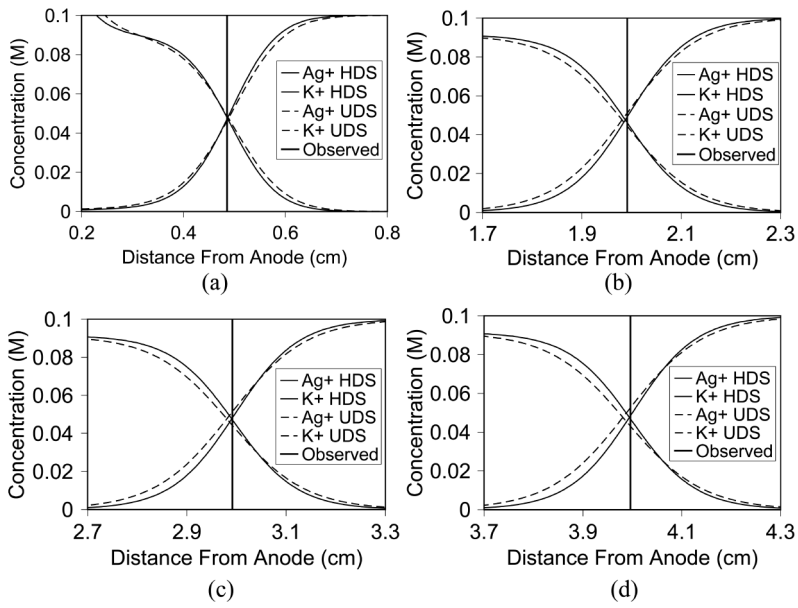

Figure 6.
The calculated moving boundary region of the Fu and Chan experimental apparatus; a) after 5 min; b) after 20 min; c) after 30 min; d) after 40 min. In each sub-figure, the vertical line represents the experimentally observed position of the boundary (boundary position was linearly interpolated from raw data)

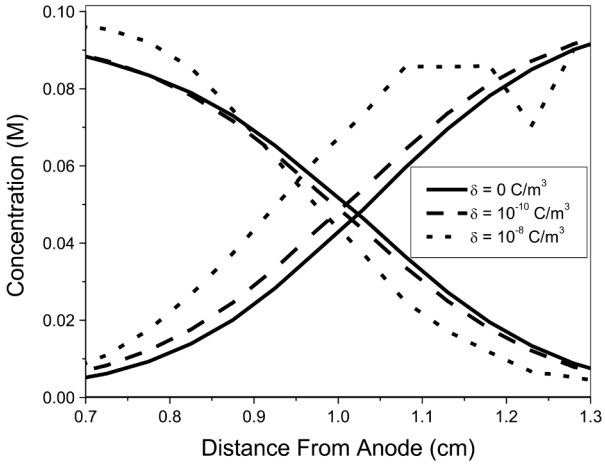

Figure 7.
The effect of charge density on the predicted moving boundary region of the Fu and Chan experiment

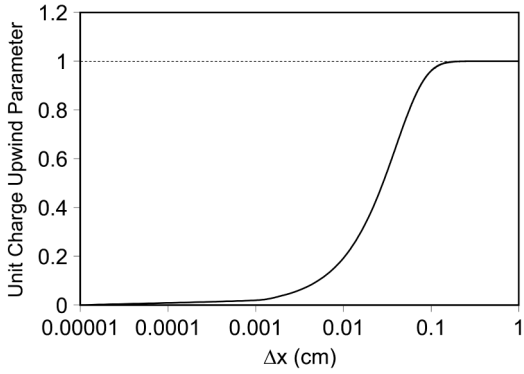

Figure 8.
The calculated unit charge upwind parameter as a function of space step size, Δx, for the model of the Fu and Chan experiment

the effect of increasing the spatial step size. As Δx was increased, the predicted upwind profile approached unity (UDS) while at very small values of Δx, the upwind parameter approached zero (CDS). As Δx decreases, the profile in the control volume approaches the linear profile predicted by differential calculus (the tangent line) and a central differencing scheme becomes appropriate. Figure 8 was generated using the mathematical model describing Fu and Chan's moving boundary experiment.

Besides having a direct impact on the value of the upwind parameter, the step size showed significant influence on the predicted concentration profile in the moving boundary region. Figure 9 shows the variation of the predicted moving boundary Ag^+/K^+ concentration profile after 10 min as the number of computational nodes used in the numerical solution is increased. The predicted concentration gradients of both K^+ and Ag^+ were predicted steeper as the number of computational nodes increased. However, the velocity of the moving boundary also decreased with increasing computational nodes. Where an inadequate number of nodes were used, a less steep concentration gradient and an increased rate of mass transport was predicted – a phenomenon that defies physical transport laws. By inspection of the electromigration

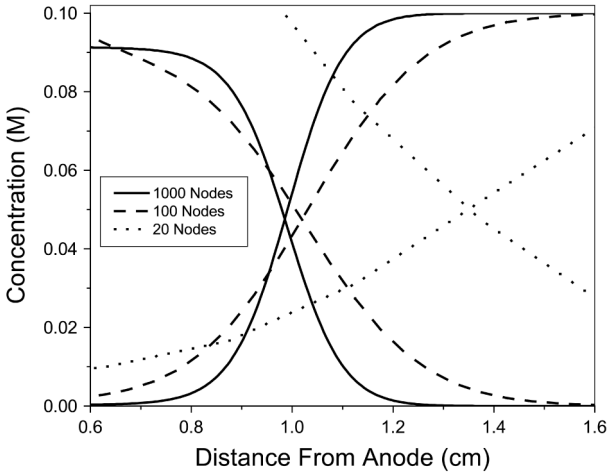

Figure 9.
The effect of step size on the predicted boundary region of the Fu and Chan experiment after 10 min

term of equation (25), the rate of mass transport due to electromigration is proportional to the concentration gradient. Therefore, the predicted profile becomes physically unrealistic as the number of nodes decrease. Furthermore, the predicted boundary position moves further away from the experimentally observed boundary position (1 cm after 10 min) (Fu and Chan, 1984).

4.3 Computational efficiency

The additional computational effort or simulation time required when using HDS rather than UDS was investigated. At each iteration, the use of HDS requires the computation of the Peclet number and the evaluation of the upwind parameter. The upwind parameter calculation is particularly expensive as it requires the computation of numerous exponential functions, each of which are computed as truncated Maclaurin series expansions. Because the additional time required to obtain a converged solution when using HDS is dependent upon both the specific mass transport problem being solved and the specifications of the computer, the computational efficiency of using HDS was investigated using the percentage increase in time, rather than the actual increase in time. The following results are therefore specific to modeling the Fu and Chan experiment but are independent of the processor speed of the computer being used. The ratio of the total number of operations that the computer is required to perform when solving the transient mass transport problem using HDS, rather than UDS, can be calculated from the following expression:

$$\text{Operations ratio} = \frac{(\text{HDS operations per iteration})(\text{HDS iterations})}{(\text{UDS operations per iteration})(\text{UDS iterations})} \tag{40}$$

The operations ratio is a measure of the increased computational effort required to use HDS rather than UDS. Because the operations required per iteration are fixed for a particular grid, variation in the value of the operations ratio is due solely to changes in the ratio of the number of iterations required to use HDS to the number of iterations required to use UDS. Figure 10 shows the percentage change in simulation time resulting when HDS, rather than UDS, is used in the mass transport solver as the

number of nodes is increased. The ease of convergence of the model can be estimated by the diagonal dominance of the transport coefficient matrix. Examining the relevant terms from equation (38), the following relationship may be written:

$$\frac{|a_P|}{|a_E| + |a_W|} \propto \frac{\Delta x^2}{P_P' \alpha} \tag{41}$$

Equation (41) seems to imply that the diagonal dominance will increase for a coarser solution grid (Δx becomes larger). However, both α and P_P' are proportional to Δx creating a competing effect of Δx upon the diagonal dominance. This competition is manifested as the peculiar functionality of the computational efficiency upon the number of nodes seen in Figure 10. In general, the results of Figure 10 show that, as the number of nodes increase, the transport coefficient matrix becomes less diagonally dominant and the additional effort required using HDS rather than UDS increases (i.e. the computational efficiency of the model decreases).

5. Conclusions

Based upon a pseudo-steady state balance between electromigration and diffusion, a novel method to interpolate interfacial properties from nodal values for electrolyte mass transport under the influence of an electrical potential field has been developed. Simulation of the moving boundary experiment of Fu and Chan (1984) provided a means of quantifying the influence of the upwind parameter on the predictions of the electrolyte mass transport model. The following conclusions can be made from this research:

- Use of HDS rather than UDS results in predictions that more closely match the experimental observations of Fu and Chan. The error between model predictions and experimental data are reduced by an average of 61 percent when HDS rather than UDS is used. Therefore, using the 1D solution of the electromigration-diffusion balance equation as a means to prescribe appropriate weighting for approximation of interfacial properties is valid for electrolyte mass transport modeling.
- Adjustment of the time step in regions where the second order gradient of the activity coefficient is significant and positive in sign will ensure that the mass

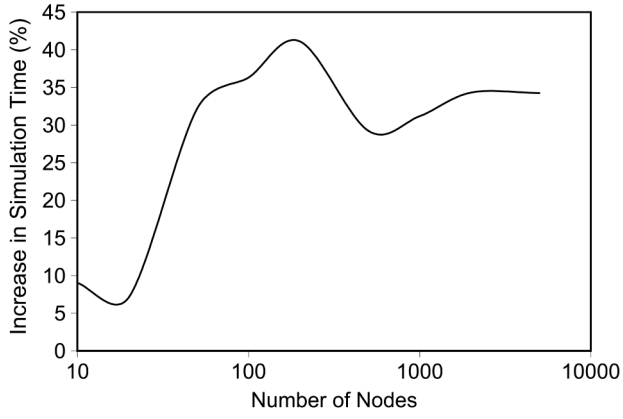

Figure 10.
The percentage increase in simulation time required when using the hybrid differencing scheme rather than the UDS as a function of the number of nodes used in the numerical solution

transport problem coupled with HDS satisfies the Scarborough criterion, a condition that checks diagonal dominance. Thus, convergence of the matrix of transport coefficients, assembled at each iteration, by the Gauss-Seidel method is guaranteed. Transport coefficients are guaranteed to be positive thus ensuring a physically realistic solution (Patankar, 1980).

- The presence of electrical charge density has a detrimental effect on the stability of the mass transport solution algorithm. As charge density increases, the solution to the steady state electromigration-diffusion equation approaches critical damping. Physically unrealistic oscillations develop in the predicted concentration profile thus altering the predicted upwind parameter. Charge density may also reduce the diagonal dominance of the coefficient matrix during the solution of the mass transport model and reduce the speed of convergence. Thus, charge density must be annihilated through direct solution of the Poisson equation for charge density or through the method proposed by Heppner *et al.* (2002).
- When the charge density and the second order gradient of the activity coefficient is negligible, the hybrid differencing scheme for electrolyte mass transport possesses the form similar to the exponential differencing formula used in computational fluid dynamics (Spalding, 1972; Raithby and Torrence, 1974). Therefore, electromigration in a stagnant, electrically neutral, infinitely dilute electrolyte under the influence of a potential gradient is analogous to convection under the influence of a pressure gradient and the use of a Peclet number-based method to estimate interfacial properties is appropriate for electrolyte mass transport.
- The Peclet number for mass transport in a non-ideal solution is affected not only by the potential gradient but also by the activity coefficient gradient. The effect of the activity coefficient gradient is a manifestation of the force exerted upon an ion to move towards regions of decreasing ionic strength. The additional term in the Peclet number formulation accounts for interactions between the ion of interest and other ions in solution.
- The computational efficiency of the mass transport model coupled with HDS is highly dependent upon the spatial step size. Thus, the percentage increase in simulation time varied between 6 and 43 percent (based on spatial step size). However, the error between the simulation results and the observations of the Fu and Chan experiment increased by as much as 87 percent by using HDS rather than UDS.
- This differencing scheme represents the first scheme developed specifically for the solution of the electromigration-diffusion equation. Previous schemes, such as the exponential scheme, power law scheme, and other schemes, have been developed for the convection-diffusion equation (refer to Patankar (1980) for a concise summary of these differencing schemes). The electromigration-diffusion equation is unique and different from the convection-diffusion equation in that its solution, if physically realistic, must satisfy the condition of charge neutrality (or very low charge density). Thus, mass transport of each ion in solution is mathematically very strongly inter-coupled with mass transport of all other ions. This unique feature is represented in the differencing scheme by the activity coefficient term in the modified Peclet number formula (equation (19b)) and by the effect of charge density upon the upwind parameter.

References

Barakat, H.Z. and Clark, J.A. (1966), "Analytical and experimental study of transient laminar natural convection flows in partially filled containers", *Proceedings of 3rd Int. Heat Transfer Conference II*, paper 57, Chicago, IL, p. 152.

Courant, R., Isaacson, E. and Rees, M. (1952), "On the solution of non-linear hyperbolic differential equations by finite differences", *Comm. Pure Appl. Math.*, Vol. 5, p. 243.

Evitts, R.W. (1997), "Modelling of crevice corrosion", PhD dissertation, University of Saskatchewan, Saskatoon, SK.

Fu, J.W. and Chan, S. (1984), "A finite element method for modelling localized corrosion cells", *Corrosion*, Vol. 40, pp. 540-4.

Gentry, R.A., Martin, R.E. and Daly, B.J. (1966), "An Eulerian differencing method for unsteady compressible flow problems", *J. Comp. Phys.*, Vol. 1, p. 87.

Heppner, K.L., Evitts, R.W. and Postlethwaite, J. (2002), "Prediction of the crevice corrosion incubation period of passive metals at elevated temperatures. Part I – mathematical model", *Canadian Journal of Chemical Engineering*, Vol. 80, pp. 849-56.

Newman, J. (1973), *Electrochemical Systems*, Prentice-Hall, Toronto, ON.

Patankar, S.V. (1980), *Numerical Heat Transfer and Fluid Flow*, Hemisphere, Washington, DC.

Patankar, S.V. and Spalding, D.B. (1970), *Heat and Mass Transfer in Boundary Layers*, 2nd ed., Intertext, London.

Raithby, G.D. and Schneider, G.E. (1980), "The prediction of surface discharge jets by a three-dimensional finite-difference model", *Journal of Heat Transfer*, Vol. 102, pp. 138-45.

Raithby, G.D. and Torrence, K.E. (1974), "Upstream-weighted differencing schemes and their application to elliptic problems involving fluid flow", *Comput. Fluids*, Vol. 2, p. 191.

Runchal, A.K. and Wolfshtein, M. (1969), "Numerical integration procedure for the steady state Navier-Stokes equations", *J. Mech. Eng. Sci.*, Vol. 11, p. 445.

Scarborough, J.B. (1958), *Numerical Mathematical Analysis*, 4th ed., Hopkins Press, Baltimore, MD.

Spalding, D.B. (1972), "A novel finite-difference formulation for differential expressions involving both first and second derivatives", *Int. J. Num. Methods Eng.*, Vol. 4, p. 551.

Walton, J.C., Cragnolino, G. and Kalandros, S.K. (1996), "A numerical model of crevice corrosion for passive and active metals", *Corrosion Science*, Vol. 38, pp. 1-18.

Watson, M.K. (1989), "Numerical simulation of crevice corrosion", PhD dissertation, University of Saskatchewan, Saskatoon, SK.

Watson, M.K. and Postlethwaite, J. (1990a), "Numerical simulation of crevice corrosion of stainless steels and nickel alloys in chloride solutions", *Corrosion*, Vol. 46, pp. 522-30.

Watson, M.K. and Postlethwaite, J. (1990b), "Numerical simulation of crevice corrosion", *Proceedings of Corrosion/90*, Las Vegas, NV, 23-27 April 1990, NACE International, Houston, TX, pp. 156:1-156:19.

Watson, M.K. and Postlethwaite, J. (1991), "Numerical simulation of crevice corrosion: the effect of the crevice gap profile", *Corrosion Science*, Vol. 32, pp. 1253-62.

Further reading

Heppner, K.L. and Evitts, R.W. (2004), "Computation of mass transport in stagnant electrolytic systems", *Dynamics of Continuous, Discrete, and Impulsive Systems – B*, Vol. 11 Nos 1/2, pp. 29-46.

(Richard W. Evitts has been a faculty member at the University of Saskatchewan since completing a PhD in 1997. He also holds two bachelor's degrees – one in chemistry and the other in Chemical Engineering. He has published numerous works dealing with both corrosion engineering and multiphase moisture transport and has been recognized for excellence in both teaching and research.

Kevin L. Heppner is currently pursuing a PhD degree at the University of Saskatchewan. He finished a bachelor's degree in Chemical Engineering at the University of Saskatchewan in 2001. He has been awarded many academic prizes and scholarships including a prestigious three-year tenure Doctoral Canada Graduate Scholarship from the Natural Sciences and Engineering Research Council of Canada (NSERC).)